MOLECULAR AND CELLULAR BIOLOGY, Jan. 2007, p. 526–540 Vol. 27, No. 2
0270-7306/07/$08.00+0 doi:10.1128/MCB.00577-06

Involvement of Specific COPI Subunits in Protein Sorting from the Late Endosome to the Vacuole in Yeast[▽]

Galina Gabriely, Rachel Kama, and Jeffrey E. Gerst*

Department of Molecular Genetics, Weizmann Institute of Science, Rehovot 76100, Israel

Received 2 April 2006/Returned for modification 30 May 2006/Accepted 1 November 2006

Although COPI function on the early secretory pathway in eukaryotes is well established, earlier studies also proposed a nonconventional role for this coat complex in endocytosis in mammalian cells. Here we present results that suggest an involvement for specific COPI subunits in the late steps of endosomal protein sorting in *Saccharomyces cerevisiae*. First, we found that carboxypeptidase Y (CPY) was partially missorted to the cell surface in certain mutants of the COPIB subcomplex (COPIb; Sec27, Sec28, and possibly Sec33), which indicates an impairment in endosomal transport. Second, integral membrane proteins destined for the vacuolar lumen (i.e., carboxypeptidase S [CPS1]; Fur4, Ste2, and Ste3) accumulated at an aberrant late endosomal compartment in these mutants. The observed phenotypes for COPIb mutants resemble those of class E vacuolar protein sorting (*vps*) mutants that are impaired in multivesicular body (MVB) protein sorting and biogenesis. Third, we observed physical interactions and colocalization between COPIb subunits and an MVB-associated protein, Vps27. Together, our findings suggest that certain COPI subunits could have a direct role in vacuolar protein sorting to the MVB compartment.

It is well accepted that COPI coat components confer the retrograde trafficking of cargo molecules from the Golgi apparatus to the endoplasmic reticulum (ER) (13, 19, 32, 40, 44, 56). The classical COPI coat consists of seven coatomer subunits: αCOP (Sec33/Ret1; 160 kDa); βCOP (Sec26; 110 kDa); β′COP (Sec27; 102 kDa); γCOP (Sec21; 98 kDa); δCOP (Ret2; 60 kDa); εCOP (Sec28; 35 kDa); and ζCOP (Ret3; 20 kDa), as well as the Arf1 small GTPase, which are conserved from yeast to mammals (56). Coatomer subunits can be divided into two subcomplexes: the B subcomplex (COPIb) composed of the α, β′, and ε subunits; and the F subcomplex (COPIf), consisting of the β, δ, γ, and ζ subunits (22, 40). Interestingly, the γ subunit of COPIf shows structural similarity to components of the clathrin adaptor, AP2 (31), while COPIb has been suggested to be clathrin-like (40). Clathrin is another multisubunit coat complex involved in Golgi apparatus-to-vacuole/lysosome transport, endocytosis, and endosomal protein sorting (36, 37, 40, 42). The COPI coat is responsible for the biogenesis and sorting of vesicles from the Golgi apparatus and their delivery to the ER via retrograde transport (38). Mutations in coatomer components directly affect retrograde trafficking, but also alter anterograde transport from the ER (18, 19, 26, 32, 60). Activation of the small GTPase, Arf1, is required for recruitment of COPI, as well as adaptors of the clathrin coat, to membranes (for review, see references 40, 42, 53, and 56). Thus, both the COPI and clathrin coats appear to have common structural properties and regulatory controls.

Studies of mammalian cells have suggested an additional function for a subset of COPI subunits upon the endocytic pathway. Mellman and colleagues demonstrated the association of certain COPI components with endosomes, identifying the α, β, β′, ε, and ζ coatomer subunits, but not the γ and δ subunits (59). Their association with endosomal membranes was GTPγS stimulated and brefeldin A sensitive, indicating that COPI binding depends upon ARF activity. Importantly, the microinjection of antibodies against βCOPI blocked infection by vesicular stomatitis virus (VSV), an envelope virus that infects cells by endocytosis. As VSV must reach the late endosome in order to enter the cytoplasm, this suggested that COPI may be involved in early to late endosome transport. Both VSV infection and the delivery of endogenous cargo proteins to late endosomes and lysosomal compartments were inhibited in CHO cells either possessing a temperature-sensitive allele of εCOP (e.g., 1d1F cells) or injected with antibodies against this subunit (15). Likewise, Gruenberg and colleagues found an inhibition in early to late endosome transport in 1d1F cells and proposed the involvement of COPI in the biogenesis of the multivesicular bodies (MVBs) in mammalian cells (29). Furthermore, they demonstrated that αCOP and βCOP recruitment to endosomes requires εCOP (29) and ARF1 (30) and is lumenal pH dependent (1). COPI was later shown to mediate Nef-induced downregulation of the human immunodeficiency virus viral receptor, CD4 (23). Nef binding of CD4 recruits the clathrin AP2 coat, resulting in clathrin-mediated endocytosis. Next, Nef binds βCOP at the early endosomes and targets CD4 to the late endosome and lysosomal compartments in an ARF1-dependent fashion (5, 23). More recently, we reported that some COPI mutants are impaired in recycling of the green fluorescent protein (GFP)-Snc1 v-SNARE from endosomes to the Golgi apparatus in yeast cells (51). Altogether, these findings support the idea of a post-Golgi apparatus role for COPI in endosomal protein sorting.

Endosomal sorting to the lysosome (in mammals) and vacuole (in yeast) consists of two principal routes. One mediates receptor internalization and downregulation via endocytosis, while the second is an integral part of the biosynthetic pathway

* Corresponding author. Mailing address: Department of Molecular Genetics, Weizmann Institute of Science, Rehovot 76100, Israel. Phone: 972-8-9342106. Fax: 972-8-9344108. E-mail: jeffrey.gerst@weizmann.ac.il.

▽ Published ahead of print on 13 November 2006.

and directs trafficking of newly synthesized hydrolases from the Golgi apparatus to the lysosome/vacuole (27). Both endosomal transport routes converge at the MVB before delivering cargo molecules to the lysosome/vacuole. Like the role for COPI in ER-Golgi apparatus retrograde transport, the requirements for protein sorting to the MVB pathway are conserved from yeast to mammals (for recent reviews, see references 28 and 46). In mammalian cells, sorting to the MVB pathway begins at the early endosome, which either matures or fuses with the late endosome and results in its appearance as a multivesicular structure (28). Transport through the MVB pathway includes protein sorting into invaginations on the surface of the endosome/MVB, subsequent intralumenal vesicle formation mediated by the MVB machinery, and fusion of the MVB with the lysosome (28, 46). Thus, the role of the MVB machinery is to sort and internalize transmembrane proteins on the limiting membrane of MVB compartment in order to incorporate them into the lumenal vesicles formed by invagination (34, 41).

Mutations in genes involved in MVB sorting and biogenesis in yeast lead to the formation of a class E vacuolar protein sorting (*vps*) phenotype, which is characterized by the aberrant enlargement of the late endosome exhibiting multilamellar structures (41, 47, 50) and the partial missorting of vacuolar carboxypeptidase Y (CPY) to the cell surface (50). Class E *vps* mutants are defective in protein sorting into, and formation of, the MVB compartment. This group belongs to a broader class of *vps* mutants, which encompasses those genes essential for endosomal and vacuolar protein sorting.

The molecular mechanism underlying MVB formation has been studied extensively (28, 46). Monoubiquitination marks proteins targeted for sorting into the MVB. The ubiquitinated substrate is recognized by Vps27, a ubiquitin receptor that is recruited to the endosomal membrane by phosphotidylinositol 3-phosphate [PI(3)P] and which initiates the process of MVB sorting (33, 35). Vps27 recruits the first of three endosome-associated complexes required for transport (e.g., ESCRT-I, -II, and -III) that act sequentially in order to sort the targeted protein into invaginations on the limiting membrane of the MVB (2, 3, 33). Yet, the precise mechanism that drives endosomal membrane invagination and intralumenal vesicle formation (the topological opposite to classical coat-dependent vesicle formation) remains to be defined.

As COPI is conserved structurally and functionally between yeast and mammals and has been shown to function upon different steps of endosomal transport in mammalian cells, we further examined its role in endosomal protein sorting in yeast. We first examined CPY secretion and found strong sorting defects in mutants with mutations in COPIb (e.g., *sec27-1*, *sec28*Δ, and *sec33-1*), but not COPIf (e.g., *sec21-1*, *sec21-2*, *ret2-1*, and *ret3-1*). Next, we found transmembrane proteins that normally target to the vacuole (e.g., CPS1, Fur4, Ste2, and Ste3) accumulate at endosomes and do not reach the vacuolar lumen in certain COPIb mutants (e.g., *sec27-1* and *sec28*Δ). We also observed the accumulation of an enlarged late endosome in those cells using the lipophilic dye FM4-64. These results parallel those described for *vps* mutants impaired in MVB sorting and vesicle formation (50). Finally, we found that Vps27 coimmunoprecipitates with all COPIb subunits and partially colocalizes with red fluorescent protein (RFP)-tagged Sec28. These observations lead us to propose the direct involvement of COPIb in endosomal protein sorting to the MVB compartment in yeast.

MATERIALS AND METHODS

Yeast strains, media, and DNA manipulation. The yeast strains used in this study are listed in Table 1. Standard rich (YPD) and synthetic complete (SC) media containing either 2% glucose or 3.5% galactose as a carbon source were used for cell growth (52). Standard methods were used for the introduction of DNA into yeast (52). Tagging of genes at their intragenomic loci with myc or GFP was performed by homologous recombination using PCR products with flanking regions of the appropriate genomic sequences and genome-tagging plasmids as templates (39).

Plasmids. Plasmids generated for this study are listed in Table 2. Plasmids pGFP-CPS1, pGFP-VPS27, and pSTE2-GFP which express *GFP-CPS1* (41), *GFP-VPS27* (35), and *STE2-GFP*, respectively, were generously provided by S. Emr (University of California, San Diego). Plasmid pSTE3-GFP, which expresses *STE3-GFP*, was kindly provided by R. Piper (University of Iowa, Iowa City). Plasmids pRS314STE2-GFP and pRS314STE2Δtail-GFP, which express *STE2-GFP* or *STE2*Δ*tail-GFP* (57), respectively, were generously provided by K. Blumer (Washington University School of Medicine, St. Louis, MO). Plasmid pGALΔBglII-CPY[1–50]GFP, which expresses $CPY^{1\text{-}50}$*-GFP*, was kindly provided by O. Deloche (Universite de Lausanne, Lausanne, Switzerland).

Fluorescence microscopy. Yeast cells expressing GFP/RFP fusion proteins were grown to mid-log phase at 26°C and examined by confocal microscopy. For induction of proteins from a *GAL* promoter (i.e., CPY-GFP), cells were grown in glucose-containing media to mid-log phase and then shifted galactose-containing media until GFP expression was observed.

FM4-64 labeling and visualization. Yeast cells grown to mid-log phase were stained with the lipophilic dye FM4-64 (Molecular Probes, Eugene, OR), basically as described previously (58). For endosomal staining, cells were incubated with 16 μM of FM4-64 on ice in the dark for 45 min. Afterwards, cells were washed twice with fresh medium and kept on ice prior to observation by confocal microscopy. To induce endocytosis and label the endosomal compartments, cells were transferred to 26°C for 10 min. For vacuolar staining, cells were pulsed with 32 μM of FM4-64 for 20 min in the dark at 26°C. Following the pulse, two chases of 20 min each in medium lacking FM4-64 at 26°C were performed. Labeled cells were observed by confocal microscopy.

Immunoblot assay for CPY and Kar2 secretion. Yeast cells were either plated or spotted (as 10-fold serial dilutions of cells) on YPD plates at 26°C and grown for 24 h prior to replica plating onto nitrocellulose filters (BA-S85; Schleicher and Schuell). The filters were then placed yeast side up, incubated on a fresh YPD plate, and grown for an additional day. The immunoblotting assay for CPY and Kar2 secretion was performed using standard procedures. Cells were removed by three washes of the membranes for 5 min each with phosphate-buffered saline. No cell lysis was observed on either plates or filters using this technique (data not shown). Filters were then blocked in 5% nonfat dry-milk in 0.1% Tween 20–phosphate-buffered saline for 1 h. After blocking, membranes were probed with polyclonal anti-CPY antibodies (1:1,000; gift of S. Emr, University of California, San Diego) or polyclonal anti-Kar2 antibodies (1:2,000; gift of C. Barlowe, Dartmouth University, Hanover, NH), and detected by ECL enhanced chemiluminescence, using anti-rabbit peroxidase-conjugated antibodies (1:10,000; Amersham Biosciences).

Separation of extracellular and intracellular forms of CPY. Five optical density at 600 nm (OD_{600}) units of yeast grown to mid-log phase was incubated in 500 μl of YPD medium containing 50 mM KPO_4, pH 5.7, for 1 h at 30°C. Then 5 μl of 1 M NaN_3 was added, and the cell cultures were cooled on ice for 10 min. Culture samples were centrifuged to separate the cells (containing the intracellular fraction; I) from the medium (containing the extracellular fraction; E). Cell pellets were resuspended in 150 μl of spheroplast-forming buffer (50 mM Tris-HCl, pH 7.4, 1.4 M sorbitol, 2 mM $MgCl_2$, 10 mM NaN_3, freshly added 40 mM β-mercaptoethanol, 0.15 mg/ml of Zymolase) and incubated by gentle shaking for 30 min at 30°C. Spheroplasts were lysed by the addition of 50 μl of 2% sodium dodecyl sulfate (SDS) and boiled for 5 min. The lysate was then centrifuged for 10 min at 20,800 × *g*, and the supernatant was removed for electrophoretic separation on acrylamide gels by SDS-polyacrylamide gel electrophoresis (SDS-PAGE). Samples taken for electrophoresis consisted of an aliquot of 0.1 OD_{600} U for the intracellular fraction and an aliquot corresponding to the volume of 0.4 OD_{600} U in culture (40 μl). SDS sample buffer was added to each sample, and the samples were separated on 8% SDS-PAGE gels. Following transfer to the nitrocellulose membranes, the blots were incubated with polyclonal anti-CPY antibodies (1:1,000; gift of S. Emr, University of California, San Diego) and proteins were visualized using ECL chemiluminescence.

TABLE 1. Yeast strains used in this study

Name[a]	Genotype	Source
SP1 (WT)	*MAT***a** *can1 his3 leu2 trp1 ura3 ade8*	M. Wigler
W303-1a (WT)	*MAT***a** *can1 his3 leu2 lys2 trp1 ura3 ade2*	J. Hirsch
BY4741 (WT)	*MAT***a** *his3Δ1 leuΔ0 met15Δ0 ura3Δ0*	Euroscarf
NY13 (WT)	*MAT***a** *ura3*	P. Novick
SEY6210 (WT)	*MATα leu2-3,112 ura3-52 his 200 trp-901 lys2-801 suc2-Δ9*	S. Emr
RSY1309 (*sec21-2*)	*MAT***a** *ura3-52 his3-Δ leu2-3,112 lys2-801 suc2-Δ9 sec21-2*	A. Spang
RDY146 (*sec27-1*)	*MATα leu2-3,112 trp1 ura3-52 sec27-1*	R. Duden
RDY241 (*sec28Δ*)	*MAT***a** *leu2 ura3 trp1 ade2 his3 lys2 sec28Δ::HIS3*	R. Duden
RDY260 (*sec33-1*)	*MATα leu2 ura3 sec33-1*	R. Duden
PC130 (*ret2-1*)	*MAT***a** *leu2 ura3 his3 lys2 suc2 ret2-1*	H. Riezman
FLY89 (*ret3-1*)	*MAT***a** *leu2 ura3 trp1 his3 suc2-Δ9 ret3-1*	H. Riezman
RSY1010 (*sec21-1*)	*MAT***a** *leu2-3,112 ura3-52 sec21-1*	R. Schekman
RSY1318 (*ret1-3*)	*MATα leu2-3,112 ura3-52 lys2-801 ret1-3*	A. Spang
Y03416 (*vps23Δ*)	*MAT***a** *his3Δ1 leuΔ0 met15Δ0 ura3Δ0 vps23Δ::kanMX*	Euroscarf
Y05588 (*vps4Δ*)	*MAT***a** *his3Δ1 leuΔ0 met15Δ0 ura3Δ0 vps4Δ::kanMX*	Euroscarf
Y05381 (*vps27Δ*)	*MAT***a** *his3Δ1 leuΔ0 met15Δ0 ura3Δ0 vps27Δ::kanMX*	Euroscarf
Y02763 (*vps28Δ*)	*MAT***a** *his3Δ1 leuΔ0 met15Δ0 ura3Δ0 vps28Δ::kanMX*	Euroscarf
Y02730 (*vps37Δ*)	*MAT***a** *his3Δ1 leuΔ0 met15Δ0 ura3Δ0 vps37Δ::kanMX*	Euroscarf
FFUY028-01D(A) (*rcy1Δ*)	*MAT***a** *his3Δ1 leuΔ0 met15Δ0 ura3Δ0 rcy1Δ::kanMX*	Euroscarf
Y01469 (*sec28Δ*)	*MAT***a** *his3Δ1 leuΔ0 met15Δ0 ura3Δ0 sec28Δ::kanMX*	Euroscarf
DKY6281 (*vam3Δ*)	*MATα his3-Δ200 leu2-3,112 ura3-52 lys2-801 suc2-9 vam3Δ::LEU2*	A. Mayer
RH268-1C (*end4-1*)	*MAT***a** *ura3 his4 leu2 bar1-1 end4-1*	H. Riezman
US1968	*MAT***a** *his3 leu2 sec27-b1 bar1Δ::hisG trp1 ura3*	U. Surana
GGY1 (*GAL-SEC28*)	*MAT***a** *his3Δ1 leuΔ0 met15Δ0 ura3Δ0 GAL1-GFP-SEC28::HIS3*	This study
GGY2 (*GAL-SEC28 vps23Δ*)	*MAT***a** *his3Δ1 leuΔ0 met15Δ0 ura3Δ0 vps23Δ::kanMX GAL1-GFP-SEC28::HIS3*	This study
GGY3 (*SEC28-GFP*)	*MAT***a** *can1 his3 leu2 lys2 trp1 ura3 ade2 SEC28-GFP::HIS3*	This study
GGY4 (*VPS27-MYC*)	*MAT***a** *can1 his3 leu2 lys2 trp1 ura3 ade2 VPS27-MYC::TRP1*	This study
GGY5 (*SEC28-GFP VPS27-MYC*)	*MAT***a** *can1 his3 leu2 lys2 trp1 ura3 ade2 SEC28-GFP::HIS3 VPS27-MYC::TRP1*	This study
GGY6 (*SEC28-GFP vps23Δ*)	*MAT***a** *his3Δ1 leuΔ0 met15Δ0 ura3Δ0 vps23Δ::kanMX SEC28-GFP::HIS3*	This study
GGY7 (*SEC21-GFP*)	*MAT***a** *can1 his3 leu2 lys2 trp1 ura3 ade2 SEC21-GFP::HIS3*	This study
GGY8 (*SEC21-GFP vps23Δ*)	*MAT***a** *his3Δ1 leuΔ0 met15Δ0 ura3Δ0 vps23Δ::kanMX SEC21-GFP::HIS3*	This study

[a] WT, wild type.

Co-IP assays. Fifteen OD_{600} U of mid-log-phase-grown yeast was lysed for each coimmunoprecipitation (co-IP), as described previously (14). The following changes were made in that cell lysis and co-IP were performed in IP buffer (1 mM EDTA, 10 mM Tris-HCl, pH 7.5, 150 mM NaCl, 0.5% Nonidet P-40) containing protease inhibitors (leupeptin, soybean trypsin inhibitor, aprotinin, and pepstatin [each at a concentration of 10 μg/ml]) and 1 mM phenylmethylsulfonyl fluoride (PMSF). For the co-IP reaction in Fig. 5A and C, 500 μg of protein derived from the total cell lysate (TCL) was diluted in IP buffer to reach a total volume of 500 μl. For the co-IP reaction in Fig. 5B, 330 μg of protein derived from the TCL was diluted in IP buffer to reach a total volume of 300 μl. Co-IP was performed with a monoclonal anti-myc antibody (5 μl per reaction; Santa Cruz Biotechnology). Coimmunoprecipitated proteins were separated on 7.5% SDS-PAGE gels followed by transfer to nitrocellulose membranes (BioTraceNT; Pall Corp.). Detection of precipitated proteins was done using monoclonal anti-myc (1:1,000), polyclonal anti-Vps27 (1:1,000; gift of S. Emr), or polyclonal anti-coatomer (1:1,000; gift of A. Spang, Max Planck Institute, Tübingen, Germany) antisera. Proteins were detected by ECL chemiluminescence, using secondary anti-mouse and anti-rabbit peroxidase-conjugated antibodies (1:10,000; Amersham Biosciences).

TABLE 2. Plasmids used in this study

Plasmid name	Gene expressed	Vector	Sites of cloning	Copy no.	Selectable marker	Source
pAD6				2μm	*LEU2*	J. Gerst
pRS426				2μm	*URA3*	J. Gerst
pADH-SEC27	*MYC-SEC27*	pAD6	SalI/SacI	2μm	*LEU2*	This study
pADH-SEC28	*MYC-SEC28*	pAD6	SalI/SacI	2μm	*LEU2*	This study
pADH-SEC33	*MYC-SEC33*	pAD6	SalI/SacI	2μm	*LEU2*	This study
pADH-SEC21	*MYC-SEC21*	pAD6	SalI/SacI	2μm	*LEU2*	This study
pADH-VSM1	*MYC-VSM1*	pAD6	SalI/SacI	2μm	*LEU2*	This study
pADH-FUR4-GFP	*HA-FUR4-GFP*	pAD54	SalI/SacI	2μm	*LEU2*	This study
pADH-GFP-SEC28	*MYC-GFP-SEC28*	pAD6	SalI/SacI	2μm	*LEU2*	This study
pADH-RFP-SEC28	*MYC-RFP-SEC28*	pAD6	SalI/SacI	2μm	*LEU2*	This study
pGFP-CPS1	*GFP-CPS1*	pRS426		2μm	*URA3*	S. Emr
pGFP-VPS27	*GFP-VPS27*	pRS426		2μm	*URA3*	S. Emr
pRS314-STE2-GFP	*STE2-GFP*	pRS314		*CEN*	*TRP1*	K. Blumer
pRS314-STE2Δtail-GFP	*STE2Δtail-GFP*	pRS314		*CEN*	*TRP1*	K. Blumer
pSTE2-GFP	*STE2-GFP*	pRS426		2μm	*URA3*	S. Emr
pGALΔBglII-CPY[1-50]GFP	CPY^{1-50}*-GFP*	pGALΔBglII		*CEN*	*URA3*	O. Deloche
pSTE3-GFP	*STE3-GFP*	pRS315		*CEN*	*LEU2*	R. Piper

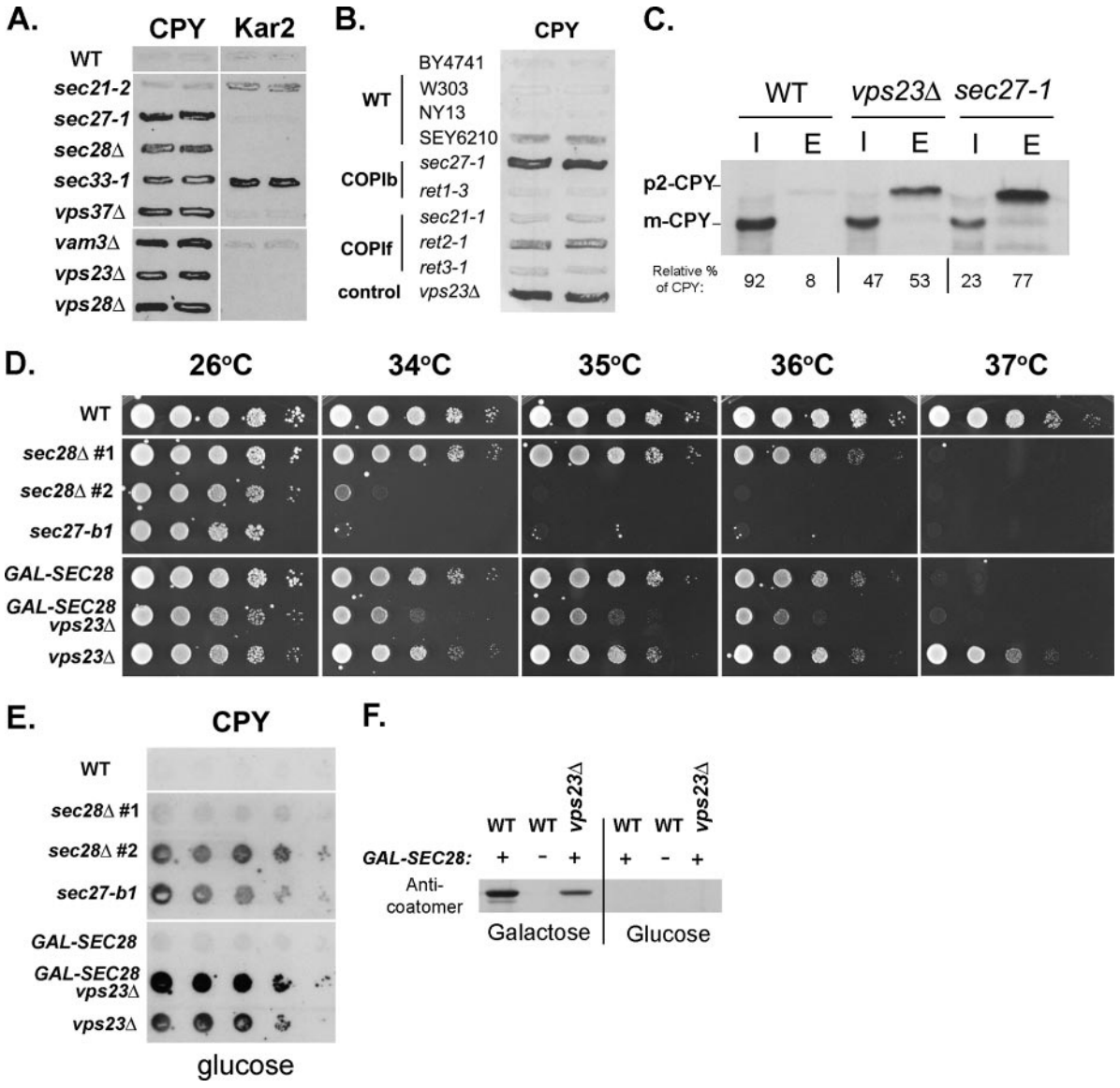

FIG. 1. Yeast strains with mutations in COPIb secrete CPY, but not Kar2. (A) Wild-type (WT) yeast (W303-1a) and strains with mutations in COPIf (*sec21-2*), COPIb (*sec27-1*, *sec28*Δ [RDY241], and *sec33-1*; gifts of R. Duden), ESCRT (*vps23*Δ, *vps28*Δ, and *vps37*Δ), and *vam3*Δ were patched onto nitrocellulose filters and grown upon solid rich medium for 1 to 2 days at 26°C. Cells secreting CPY and Kar2 were identified by immunodetection (see Materials and Methods). Both the *vam3*Δ and ESCRT mutants served as positive controls for CPY secretion. (B) Various wild-type cells and COPI mutants do not secrete CPY. Wild-type yeast (BY4741, W303-1a, NY13, and SEY6210) and strains with mutations in COPIb (*sec27-1* and *ret1-3*), COPIf (*sec21-1*, *ret2-1*, and *ret3-1*), and ESCRT (*vps23*Δ) were patched onto nitrocellulose filters and treated as described in the legend to Fig. 4A. (C) p2-CPY is secreted into the medium from a COPI mutant. Five OD_{600} U of wild-type yeast (BY4741), ESCRT (*vps23*Δ), and COPIb (*sec27-1*) was grown in YPD medium containing 50 mM KPO_4, pH 5.7, for 1 h at 30°C. Cultures were harvested by centrifugation to separate the intracellular (I; cells) and extracellular (E; medium) fractions. The fractions were treated as detailed in Materials and Methods, and aliquots of each were separated by SDS-PAGE. The positions of the precursor (p2-CPY) and mature (m-CPY) forms of CPY are indicated. Relative amounts (in percent) of the secreted (p2-CPY) and intracellular (m-CPY) forms of CPY for each strain, as calculated using densitometry, are presented below the Western blot. (D) Growth sensitivity of various COPIb strains. Wild-type yeast (BY4741) and ESCRT (*vps23*Δ) and COPIb (*sec27-b1*, *sec28*Δ #1 [Y01469] and *sec28*Δ #2 [RDY241]) mutant cells were grown on glucose-containing medium; and yeast strains with a galactose-inducible *SEC28* allele (*GAL-SEC28* and *GAL-SEC28 vps23*Δ) were maintained on galactose-containing medium prior to shifting to glucose-containing medium for 20 h. Cells were then diluted serially (10-fold dilutions) and plated onto solid medium. Cells were grown at various temperatures (26°C to 37°C, as indicated) for 2 days. (E) COPIb strains secrete different levels of CPY. The same strains as shown in panel D were grown at 26°C on a nitrocellulose filter on a YPD plate. CPY detection was performed as described for panel A. (F) Suppression of *SEC28* expression in glucose-containing media. Wild-type and *vps23*Δ yeast cells bearing *GAL-SEC28* (GGY1 and GGY2, respectively) were grown on either galactose- or glucose-containing medium for 20 h, lysed, and subjected to Western blot analysis using anticoatomer antibodies.

RESULTS

Secretion of CPY from COPIb mutants. To test the general requirement for COPI in late endosomal protein sorting, we examined the secretion of CPY, a vacuolar hydrolase that is released to the extracellular space from cells defective in Golgi apparatus-endosome transport (2, 11, 50). To do this, we employed temperature-sensitive mutants of COPI that do not exhibit strong defects in anterograde transport at permissive

TABLE 3. Summary of vacuolar protein sorting phenotypes in COPI mutants

Strain type	COPI subunit	Source	CPY secretion	Vacuolar delivery of GFP-tagged protein:			
				Fur4	Ste2	Ste3	CPS1
Wild type (W303-1a)		J. Hirsch	−	+	+	+	+
*vps23*Δ		Euroscarf	+++	−	−	−	−
*vps28*Δ		Euroscarf	+++	ND[a]	ND	ND	ND
*vps37*Δ		Euroscarf	+++	−	ND	ND	ND
sec27-1	COPIb	R. Duden	+++	−	−	−	−
sec27-1b	COPIb	U. Surana	++	+	+	ND	ND
*sec28*Δ (RDY241)	COPIb	R. Duden	++	−	−	−	−
*sec28*Δ (Y01469)	COPIb	Euroscarf	−	+	ND	+	ND
*sec28*Δ *(GAL1-SEC28)*	COPIb	This study	−	+	ND	+	ND
sec33-1	COPIb	R. Duden	++	+/−[b]	+/−[b]	+	−
ret1-3	COPIb	A. Spang	−	+	+	+	+
sec21-2	COPIf	A. Spang	−	+	+[c]	+	+
sec21-1	COPIf	R. Schekman	−	+[c]	+	+	+
ret2-1	COPIf	H. Riezman	+	+	+	+	+
ret3-1	COPIf	H. Riezman	−	+	+	+	+

[a] ND, not determined.
[b] GFP-tagged vacuolar markers localized to compartments adjacent to the vacuole; however, a portion of those proteins was found in the vacuolar lumen.
[c] GFP-tagged vacuolar proteins mainly targeted to the vacuolar interior, while the rest accumulated as small puncta throughout the cytoplasm.

temperatures: *sec27-1* cells, wherein CPY exit from the ER is slightly affected (19); *sec28*Δ (20) and *sec21-2* (38) cells, which are unaffected; and *sec33-1* cells, wherein the ER form of CPY (p1-CPY) accumulates (60). We employed an immunoblot assay to detect CPY secretion onto nitrocellulose filters using anti-CPY antibodies. This allows for easy and reliable detection of general endosomal sorting defects in yeast cells (12). This assay has been widely used to isolate *vps* mutants that secrete CPY (7). In wild-type cells, p2-CPY is delivered to the vacuole from the Golgi apparatus, where it undergoes maturation (to m-CPY) and serves as a proteolytic enzyme in degradation processes. In contrast, the p2 form of CPY is partially missorted and secreted outside the cell in *vps* (including class E) mutants, which are impaired in late endosomal protein sorting (9). By employing this immunoblot assay, we found that *sec27-1* cells secreted CPY at levels similar to deletion mutants of the ESCRT-I subunits (e.g., *vps23*Δ, *vps28*Δ, and *vps37*Δ cells), as well as a deletion of the vacuolar t-SNARE, Vam3 (16), at 26°C (Fig. 1A, B, and E; and Table 3). We observed slightly less CPY secretion from *sec28*Δ and *sec33-1* cells (Fig. 1A). In contrast to the COPIb mutants, neither various wild-type strains (e.g., BY4741, W303-1a, and NY13) nor cells bearing mutations in COPIf subunits (e.g., *sec21-1*, *sec21-2*, and *ret3-1*) secreted CPY. Although wild-type strain SEY6210 and the *ret2-1* mutant strain secreted a small portion of CPY (perhaps reflecting some defect in vacuolar protein sorting), the amount of the secreted protein was much lower than that seen from *sec27-1* and *vps23*Δ cells (Fig. 1B and Table 3). Together, these results indicate that some of COPI mutants have defects in post-Golgi apparatus sorting and endosomal transport.

In order to characterize the type of secreted CPY in the COPIb (*sec27-1*) strain, we separated the medium from the cells and examined the protein using Western blotting. After 1 h of cell incubation at 30°C, p2-CPY was secreted into the medium from *sec27-1* and *vps23*Δ mutants, but not from wild-type cells (Fig. 1C). Using densitometry, we calculated the relative amounts of secreted p2-CPY versus intracellular m-CPY for each cell type. In *sec27-1* cells, 77% of CPY (p2-CPY) was secreted while in the *vps23*Δ mutant, 53% of p2-CPY was found in the extracellular fraction. Correspondingly, the amount of intracellular m-CPY in *sec27-1* cells appeared to be lower than that in *vps23*Δ cells (23% versus 47%, respectively). This may indicate that the defect in CPY sorting is more severe in the *sec27-1* mutant than in *vps23*Δ cells.

We also examined CPY secretion from a *sec28*Δ deletion mutant in the Euroscarf (BY4741) background, although we did not observe as much secretion of CPY as strain RDY241 (*sec28*Δ #2, Fig. 1E and Table 3). Assuming that variation might occur due to adaptive responses to the deletion of *SEC28* in either strain, we prepared a conditional Sec28-deficient strain. We inserted an inducible *GAL1* promoter upstream of the *SEC28* locus by homologous recombination. This insertion also introduced *GFP* at the amino-terminal end of *SEC28*. Cells were grown on galactose-containing medium prior to shifting to glucose-containing medium to turn off *SEC28* expression. Since the deletion of *SEC28* is temperature sensitive (20), we first examined whether the *GAL-SEC28* (GGY1) strain is temperature sensitive on glucose-containing medium. We found that this strain was unable to grow at 37°C on glucose-containing medium (Fig. 1D) but was able to grow on galactose-containing medium (data not shown). Next, we confirmed that Sec28 expression was absent in cells grown on glucose using Western blot analysis (Fig. 1F). However, *GAL-SEC28* cells grown on glucose were found to secrete very little CPY at permissive temperatures (26°C; Fig. 1E), indicating that *SEC28* depletion alone did not yield substantial CPY missorting in our wild-type background. We next examined the contribution of Sec28 function to cells partially defective in CPY trafficking to the vacuole. We employed a mutant deficient in an ESCRT-I component (*vps23*Δ), which is defective in MVB protein sorting, and created a *GAL-SEC28 vps23*Δ strain (GGY2). We found that the double mutation led to more temperature-sensitive growth at elevated temperatures and increased levels of CPY secretion at 26°C on glucose-containing medium in comparison to the *vps23*Δ mutation alone (Fig. 1D). These observations indicate a possible genetic interaction

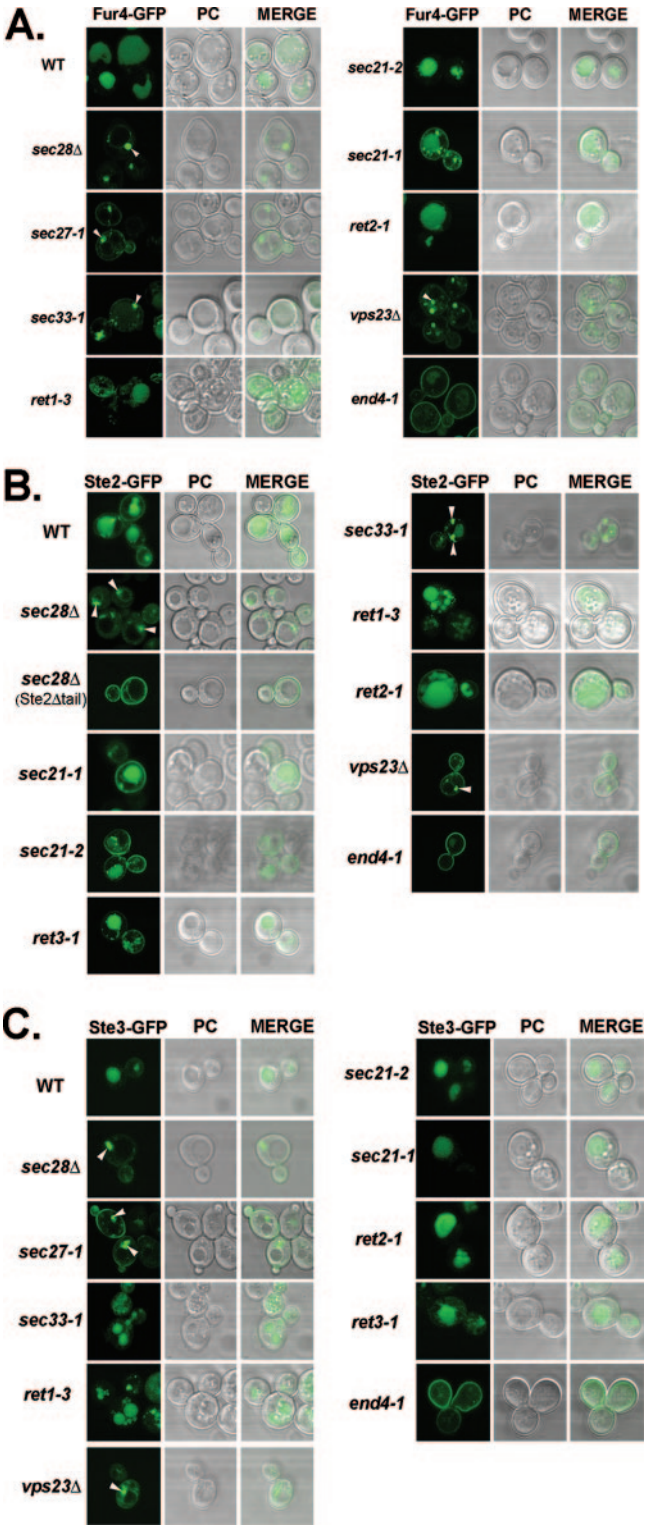

FIG. 2. Vacuole-targeted transmembrane proteins accumulate on endosomes and do not reach the vacuolar lumen in certain COPI mutants. (A) Fur4 does not target to the vacuolar lumen in COPIb mutants. Wild-type (WT) yeast (W303-1a) and strains with mutations in COPIf (*sec21-1*, *sec21-2*, and *ret2-1*), COPIb (*sec27-1*, *sec28*Δ [RDY241], *sec33-1*, and *ret1-3*), ESCRT (*vps23*Δ), and endocytosis (*end4-1*) were transformed with a multicopy plasmid expressing *FUR4-GFP* (pADH-FUR4-GFP) and examined by confocal microscopy. Both phase-contrast microscopy (PC) and merged (MERGE) panels are indicated. (B) Ste2 does not target to the vacuolar lumen in a COPIb mutant. Wild-type yeast (W303-1a) and a COPIb mutant (*sec28*Δ [RDY241]) were transformed with a single-copy plasmid producing either Ste2-GFP (pRS314-STE2-GFP) or Ste2Δtail-GFP (pRS314-STE2Δtail-GFP; Ste2Δtail). Strains with mutations in COPIf (*sec21-1*, *sec21-2*, *ret2-1*, and *ret3-1*), COPIb (*sec33-1* and *ret1-3*), ESCRT (*vps23*Δ), and *END4* (*end4-1*) were transformed with a multicopy plasmid expressing *STE2-GFP* (pSTE2-GFP). Arrows indicate the position of endosomal compartments adjacent to the vacuole in which GFP-tagged markers accumulate. (C) Ste3 does not target to the vacuolar lumen in COPIb mutants. Wild-type yeast (W303-1a) and strains with mutations in COPIf (*sec21-1*, *sec21-2*, *ret2-1*, and *ret3-1*), COPIb (*sec27-1*, *sec28*Δ [RDY241], *sec33-1*, and *ret1-3*), ESCRT (*vps23*Δ), and *END4* (*end4-1*) were transformed with a single-copy plasmid expressing *STE3-GFP* (pSTE3-GFP) and examined by confocal microscopy. Arrows indicate the position of endosomal compartments adjacent to the vacuole in which Ste3-GFP accumulates.

between *SEC28* and *VPS23* and further support our hypothesis on the involvement of Sec28 in vacuolar protein sorting. In addition, we found that another *SEC27* allele, *sec27-b1*, which was isolated as a mutant unable to localize proteins involved in budding at bud sites (43), secreted elevated levels of CPY at 26°C (Fig. 1E and Table 3). Together, these observations indicate significant phenotypic variations among COPI mutants obtained from different sources. This could potentially explain why COPI subunits were not previously identified as *vps* mutants.

Because COPI facilitates ER-Golgi apparatus retrograde transport, we examined COPIb mutants for retention of an ER resident protein, Kar2, at 26°C. In wild-type cells, Kar2 is retrieved from the Golgi apparatus back to the ER by COPI vesicles; however, defects in retrograde transport lead to Kar2 secretion (54). We next examined Kar2 secretion onto filters from these cells at permissive temperatures (26°C), under the same conditions in which CPY was secreted. We observed that *sec21-2* cells secrete small amounts of Kar2, while *sec33-1* cells secrete significantly detectable amounts at 26°C (Fig. 1A). This contrasts with wild-type cells, class E *vps* mutants, *vam3*Δ cells, and the other COPIb mutants (e.g., *sec27-1* and *sec28*Δ [RDY241]), which did not secrete Kar2. In the case of *sec27-1* and *sec28*Δ cells, this suggests that defects in CPY protein sorting occur under conditions in which Golgi apparatus-ER transport is unaffected.

Vacuole-targeted transmembrane proteins accumulate on endosomes adjacent to the vacuole in certain COPI mutants. To further investigate whether vacuolar protein sorting is generally affected in COPI mutants, we applied a microscopy approach and examined the localization of a number of proteins that undergo trafficking to the vacuole (Fig. 2 and 3). We first examined the localization of transmembrane proteins known to target to the vacuole (Fig. 2 and 3A). These proteins (i.e., CPS1, Fur4, Ste2, and Ste3) reach the vacuolar lumen by means of the MVB internalization and vacuolar fusion machinery in wild-type cells, but may accumulate on the endosomal compartment adjacent to the vacuole in class E *vps* mutants (10, 34, 41, 55). Proteins which do not undergo internalization at the limiting membrane of MVB are delivered to the limiting membrane of the vacuole, where they remain stabilized (33).

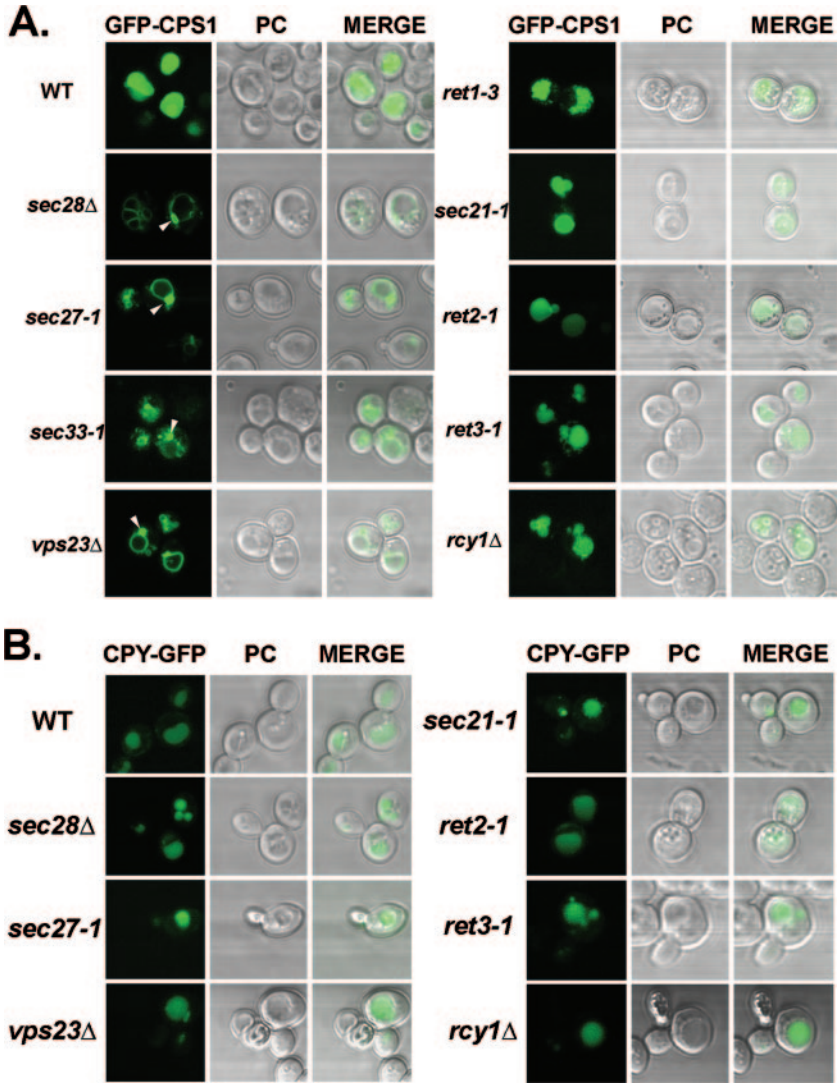

FIG. 3. CPS1 localization is impaired, although CPY^{1-50}GFP localizes normally, in certain COPI mutants. (A) CPS1 does not target to the vacuolar lumen in COPIb mutants. Wild-type (WT) yeast (W303-1a) and strains with mutations in COPIf (*sec21-2*, *ret2-1*, and *ret3-1*), COPIb (*sec27-1*, *sec28*Δ [RDY241], *sec33-1*, and *ret1-3*), ESCRT (*vps23*Δ), and *RCY1* (*rcy1*Δ) were transformed with a multicopy plasmid expressing *GFP-CPS1* (pGFP-CPS1) and examined by confocal microscopy. Both phase-contrast microscopy (PC) and merged (MERGE) panels are indicated. (B) CPY-GFP localizes to the vacuole in COPIb mutants. Wild-type yeast (W303-1a) and strains with mutations in COPIb (*sec27-1* and *sec28*Δ [RDY241]), COPIf (*sec21-1*, *ret2-1*, and *ret3-1*), ESCRT (*vps23*Δ), and *RCY1* (*rcy1*Δ) were transformed with a single-copy plasmid expressing CPY^{1-50}*-GFP* (pGALΔBglII-CPY[1–50]GFP) and examined by confocal microscopy.

We first examined delivery of the lumenal vacuolar resident enzyme, CPS1, by monitoring localization of a GFP-tagged form of CPS1 (34, 41). We found that like an ESCRT-I mutant (*vps23*Δ), GFP-CPS1 is not delivered to the vacuolar lumen in COPIb mutants (Fig. 3A). Notably, in *sec27-1* and *sec28*Δ cells (those used in Fig. 1A), GFP-CPS1 was present on the limiting membrane of the vacuole and in large punctate structures located adjacent to the vacuole. This contrasts with wild-type cells or *rcy1*Δ cells, which are deficient in early endosome-Golgi protein recycling (24), wherein GFP-CPS1 labeling is present in the vacuolar lumen (Fig. 3A). Likewise, GFP-CPS1 localized to the vacuolar lumen in COPIf mutants (e.g., *sec21-1*, *ret2-1*, and *ret3-1*) (Fig. 3A), suggesting that they have no effect upon CPS1 sorting to MVB pathway. Finally, we examined two alleles of αCOP (*sec33-1* and *ret1-3*), a COPIb component, and found that GFP-CPS1 sorting was partially affected in *sec33-1* cells, but was not affected in *ret1-3* cells. Together, these results indicate that only mutations in COPIb subunits have an effect upon CPS1 sorting, but they may be allele specific.

Next, we examined the localization of GFP-tagged Fur4, a protein that resides on the plasma membrane, but is degraded in the vacuole through the MVB pathway (34) or recycled through a late endosome back to the cell surface (10). As expected, Fur4-GFP yields labeling of the vacuolar lumen in wild-type cells, but localizes to the plasma membrane in an endocytosis-defective mutant, *end4-1* (49) (Fig. 2A). In contrast, Fur4-GFP is present on the plasma membrane and ac-

cumulates in intracellular compartments in specific COPIb mutants (*sec27-1* and *sec28*Δ), as well as the *vps23*Δ (Fig. 2A) and *vps37*Δ (data not shown) ESCRT-I mutants (Fig. 2A). A partial defect in Fur4-GFP delivery to the vacuole was observed in *sec21-1* cells, but was not observed in the *sec21-2* COPIf and *ret1-3* COPIb mutants (Fig. 2A and Table 3), which show defects in anterograde ER-to-Golgi apparatus transport at 26°C.

We then examined the localization of GFP-tagged versions of Ste2 and Ste3, which are mating factor receptors that undergo downregulation through internalization from the plasma membrane and delivery to the vacuole by sorting to the MVB vesicles (34). We found that Ste2-GFP expressed from a single-copy plasmid labeled the vacuole and plasma membrane in wild-type cells, but was mainly concentrated in a large punctate structure adjacent to the vacuole in the *sec28*Δ mutant (RDY241; Fig. 2B). In contrast, *sec28*Δ cells expressing a truncated version of Ste2-GFP, which does not undergo internalization from the cell surface (Ste2Δtail) (57), yielded typical plasma membrane labeling. This demonstrates that Ste2-GFP requires internalization to accumulate at a compartment adjacent to the vacuole in the COPIb mutant. Ste2-GFP expressed from a multicopy plasmid in *sec33-1* cells was partially impaired in its delivery to the vacuole. In contrast, in *sec21-1*, *sec21-2*, *ret2-1*, *ret3-1*, and *ret1-3* cells Ste2-GFP trafficked properly. When expressed from a single-copy plasmid, Ste3-GFP was unable to reach the vacuole in either *sec28*Δ (RDY241) or *sec27-1* mutants (Fig. 2C), but was trafficked properly in *sec33-1* and *sec21-2* cells. In *end4-1* cells, which are defective in endocytosis (49), both Ste2-GFP (Fig. 2B) and Ste3-GFP (Fig. 2C) labeled the plasma membrane but were unable to be internalized, as expected. Finally, in the control class E *vps* mutant (*vps23*Δ), both Ste2-GFP (Fig. 2B) and Ste3-GFP (Fig. 2C) accumulated at compartments adjacent to the vacuole, similar to what was observed in the *sec28*Δ and *sec27-1* COPIb mutants.

Together, these results imply that specific mutations in COPIb subunits missort transmembrane proteins to either the limiting membrane of the vacuole or a large late endosomal compartment adjacent to the vacuole, in the case of CPS1 (Fig. 3A), or endosomal compartments adjacent to the vacuole, in the case of recycling plasma membrane proteins, Fur4 (Fig. 2A), Ste2 (Fig. 2B), and Ste3 (Fig. 2C). While our immunoblot assay (Fig. 1A, B, and E) indicated that endosomal transport is affected in some COPI mutants, the mislocalization of various vacuolar markers clearly demonstrates that a late step in vacuolar protein sorting is impaired therein.

The CPY-GFP soluble vacuolar hydrolase localizes normally in COPI mutants. The fact that vacuole-targeted transmembrane proteins are mislocalized in ESCRT-I and certain COPIb mutants suggests that COPIb may participate in the process of MVB protein sorting and/or biogenesis. To examine this further, we determined the localization of a soluble endocytic cargo whose transport does not depend on the MVB internalization, namely CPY. Although CPY is secreted in part from certain COPIb mutants (Fig. 1 and Table 3), we examined whether an intracellular fraction of this soluble vacuolar marker reaches the vacuole. Since CPY delivery to the vacuole does not require internalization into the MVB (50), unlike CPS1, it has a possibility of reaching the vacuolar lumen due to accumulation of m-CPY even in the intracellular fraction of class E *vps* mutants (2, 45). We examined CPY delivery by monitoring the localization of a GFP-tagged and truncated form of CPY (CPY^{1-50}-GFP) (17) in COPIb and other mutants (Fig. 3B). We found that CPY^{1-50}GFP labeled the vacuolar lumen in both *sec27-1* and *sec28*Δ (RDY241) cells, as well as in COPIf (*sec21-1*, *ret2-1*, and *ret3-1*) mutants, an ESCRT-I mutant (e.g., *vps23*Δ), and *rcy1*Δ cells. Thus, while a portion of CPY is secreted from COPIb mutants (Fig. 1A, B, C, and E), another portion is delivered properly. These findings are consistent with previous observations showing that CPY processing is normal in both *sec27-1* and *sec28*Δ cells at permissive temperatures (20, 38). The delivery of soluble vacuolar proteins to the vacuole in COPIb mutants, in contrast to the accumulation of transmembrane proteins on the class E compartment therein, further supports the idea of COPIb involvement in the MVB sorting pathway.

Certain COPIb mutants have enlarged late endosomal compartments. We next examined whether the COPIb mutants accumulate an enlarged late endosome (class E compartment) similar to the established class E *vps* mutants (2, 3, 50). To determine this, we performed vital staining of vacuoles and endosomes with the lipophilic styryl dye FM4-64 (58). Addition of FM4-64 to yeast leads to dye incorporation into the plasma membrane, which is subsequently endocytosed and transported via endosomal transport intermediates to the vacuole. We examined endosomal staining by pulse-labeling with FM4-64 on ice and a short chase at 26°C, as well as vacuolar labeling by pulse-chase incubation at 26°C (Fig. 4A). We found that in wild-type cells, FM4-64 labeled multiple small intracellular compartments (Fig. 4A, left panels), which correspond to endosomes, after pulse-labeling on ice and the chase at 26°C, as previously described (58). In contrast, certain COPIb mutants (e.g., *sec27-1* and *sec28*Δ [RDY241]) tended to have single large punctate structures located adjacent to the vacuole (Fig. 4A). A similar type of labeling was observed in control *vps23*Δ cells (Fig. 4A), which are known to have enlarged late endosomes (*vps* class E compartment) (4). In pulse-chase experiments performed at 26°C, vacuolar labeling was observed in wild-type cells, as well as in the COPIb and *vps23*Δ mutants (Fig. 4A, right panels). However, single large punctate structures (i.e., late endosomes) were still observed adjacent to the vacuole in the *sec27-1*, *sec28*Δ (RDY241), and *vps23*Δ cells after the chase period. No significant defects in FM4-64 endosomal and vacuolar labeling were obvious in either *sec33-1* or the *sec21-2* mutants. Thus, altered FM4-64 labeling is exhibited in specific COPIb mutants and the large labeled structure located adjacent to the vacuole closely resembles the class E compartment seen in certain *vps* mutants (50).

Next, we labeled COPIb cells expressing either GFP-CPS1 or Fur4-GFP with FM4-64, by pulse-chase labeling at 26°C (Fig. 4B). This allowed us to determine whether FM4-64 accesses the same enlarged late endosomal compartment in which Fur4 and CPS1 accumulate (Fig. 2A and 3A, respectively). As expected, we found both GFP-CPS1 and Fur4-GFP colocalized with FM4-64 in an enlarged compartment adjacent to the vacuole in both *sec27-1* and *sec28*Δ cells (Fig. 4B). This colocalization was observed in all cells that had an obvious class E phenotype. This demonstrates that the loss of COPIb function leads to the accumulation of vacuole-bound cargoes

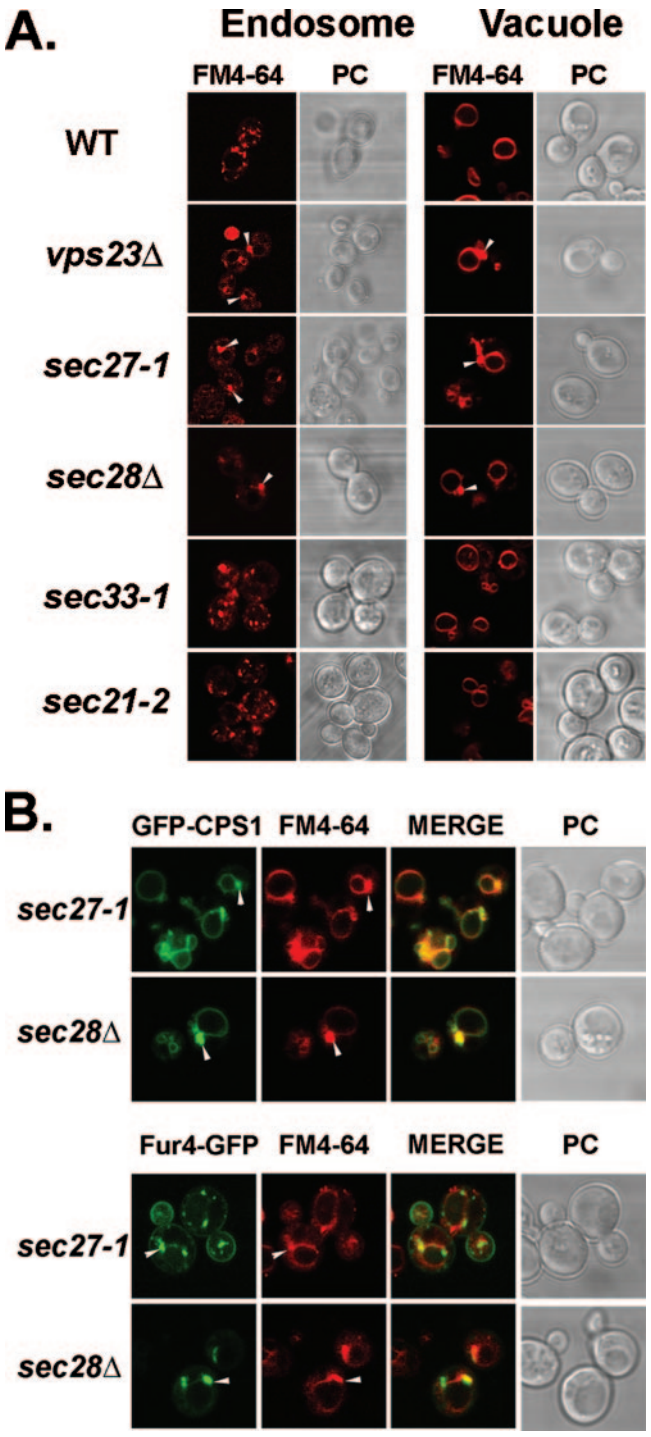

FIG. 4. FM4-64 labeling of an enlarged late endosome in certain COPI mutants. (A) FM4-64 staining of endocytic membranes in COPIb mutants. Wild-type (WT) cells (W303-1a) and mutants in COPIf (*sec21-2*), COPIb (*sec27-1*, *sec28*Δ, and *sec33-1*), and ESCRT (*vps23*Δ) were grown to mid-log phase and subjected to endosomal and vacuolar labeling with FM4-64 to visualize these organelles (see Materials and Methods). Arrows indicate positions of class E compartment in which FM4-64 accumulates. Phase-contrast microscopy (PC) panels are indicated. (B) Colocalization of FM4-64 with accumulated transmembrane proteins in COPIb mutants. *sec28*Δ (RDY241) and *sec27-1* yeast cells expressing GFP-CPS1 or Fur4-GFP proteins were stained with FM4-64 by pulse-chase labeling at 26°C. Both phase-contrast microscopy (PC) and merged (MERGE) panels are indicated.

in the enlarged late endosome. This effect is not likely to be indirect (i.e., due to defects in retrograde ER-Golgi apparatus transport) since the protein markers examined in this study reached the endosomal compartments and do not accumulate at early compartments (e.g., ER or Golgi apparatus) within the cells. However, we cannot rule out the possibility that a COPI-mediated endosomal recycling event might also alter protein sorting into vesicles.

Vps27 coimmunoprecipitates with COPIb subunits. The fact that COPIb and class E *vps* mutants have a similar phenotype suggested that COPIb may be involved directly in the MVB sorting pathway. To address this, we examined whether COPIb subunits are able to bind to Vps27, a protein of the late endosome/MVB that is involved in early steps of MVB biogenesis. We performed co-IP experiments between myc-tagged subunits of COPIb (e.g., myc-Sec27, myc-Sec28, and myc-Sec33) and GFP-Vps27, using anti-myc antibodies (35) (Fig. 5A). These myc-tagged constructs were functional, given their ability to rescue their respective temperature-sensitive mutations (data not shown). In addition, we used a *vps23*Δ mutant as the strain background as a block in cargo internalization presumably locks the recruited components of MVB machinery onto the endosomal membrane (2, 3, 8, 33).

As shown in Fig. 5A, all three tagged COPIb subunits were expressed well and had mobilities on SDS-PAGE gels corresponding to their expected molecular weights, although some degradation products were observed in the lysates of myc-Sec27- and myc-Sec33-producing cells. The latter are probably due to proteolysis during sample preparation. Importantly, GFP-Vps27 coimmunoprecipitated with all three COPIb subunits (Sec27, Sec28, and Sec33), but was not evident in precipitates obtained from cells expressing vector alone. This interaction was also observed in wild-type cells (Fig. 5B and C), indicating the ability of Vps27 to bind to COPIb under normal conditions. Based upon our coimmunoprecipitation data, we estimated by densitometry that 2 to 3% of cellular Vps27 was precipitated by the COPI subunits. Such a low level of association between these COPI components and Vps27 may indicate either a weak interaction between these proteins or, alternatively, that only a small portion of COPI is involved in vacuolar protein sorting. It is also possible that the interaction between COPI components and Vps27 may not be direct, but is mediated by another protein. A nonrelevant myc-tagged protein, Vsm1, did not precipitate Vps27 (Fig. 5C), indicating that COPI subunits precipitate Vps27 specifically. We note that overexpressed GFP-Vps27, but not native Vps27, was observed in these immunoprecipitation experiments, which could be due to low sensitivity of the anti-Vps27 antiserum. In addition, we note that COPI protein-protein interactions are apparently maintained in these cells, as myc-Sec27 and myc-Sec28 were able to coimmunoprecipitate both native and myc-Sec33 protein. To begin characterizing the molecular requirements for the COPI-Vps27 interaction, we examined whether Sec33 could bind Vps27 in cells lacking a nonessential COPI component (*sec28*Δ cells). As can be seen in Fig. 5B, GFP-Vps27 could be precipitated via myc-Sec33 in *sec28*Δ cells as efficiently as in wild-type and *vps23*Δ cells, indicating that Sec28 is not essential for their interaction. We also examined whether a COPIf subunit, Sec21, is able to precipitate Vps27, but we could not observe the interaction (Fig. 5B). As the

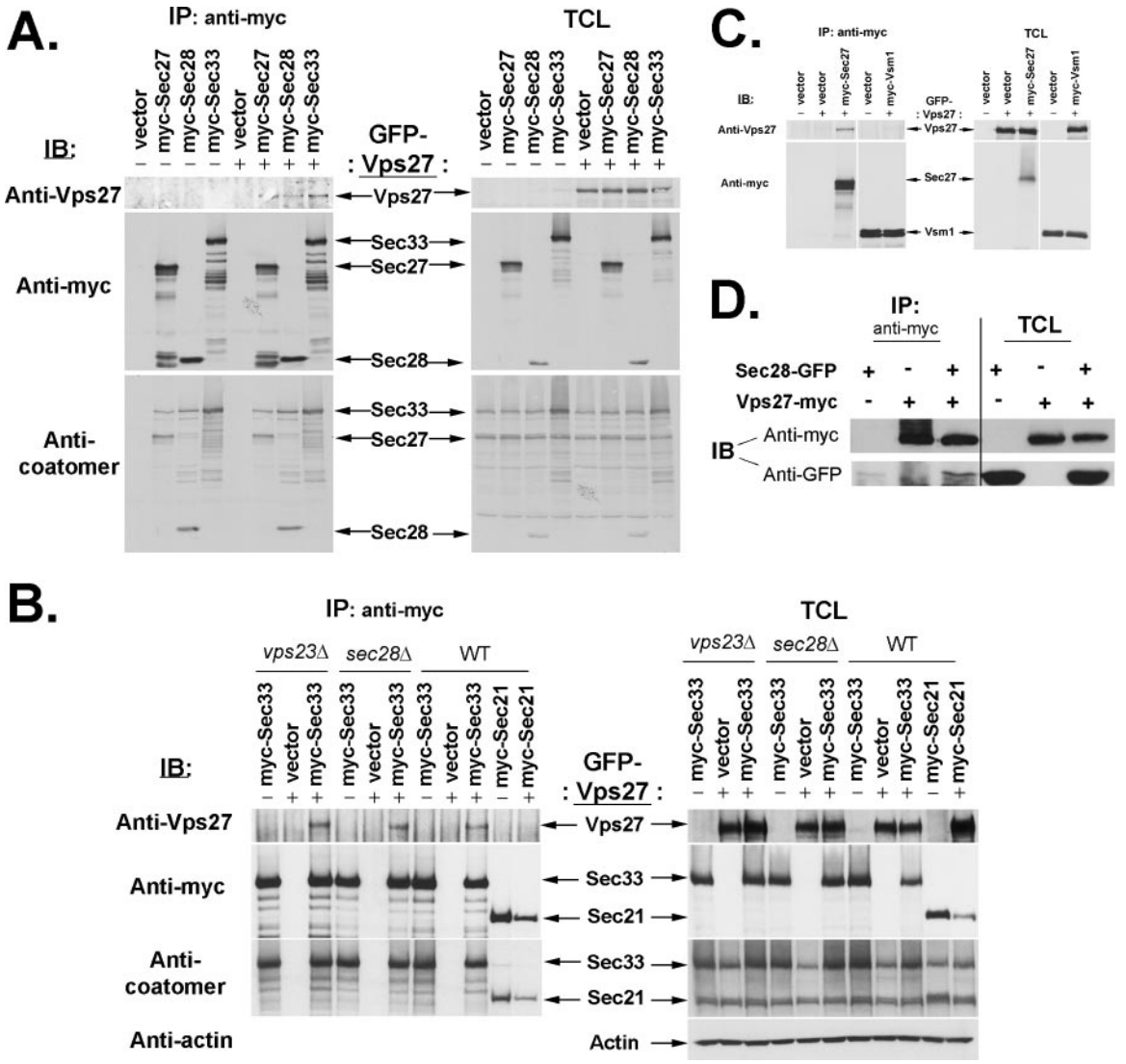

FIG. 5. Vps27 binds to subunits of COPIb. (A) Coimmunoprecipitation of GFP-Vps27 with COPIb. Class E *vps* mutant yeast (*vps23*Δ) bearing multicopy plasmids expressing *myc-SEC27* (pADH-SEC27), *myc-SEC28* (pADH-SEC28), or *myc-SEC33* (pADH-SEC33), together with a second plasmid expressing *GFP-VPS27* (pGFP-VPS27), were lysed and subjected to immunoprecipitation (IP) with anti-myc antibodies. Detection of the precipitated proteins in immunoblots (IB) was performed with anti-Vps27 (1:1,000), anticoatomer (1:1000), or anti-myc (1:1,000) antibodies. "Vector" indicates cells transformed with an empty vector (pAD6). −, cells lacking the GFP-Vps27 protein; +, cells producing the GFP-Vps27 protein. Samples of the TCL are shown (50 μg protein/lane). (B) Sec33 interacts with Vps27 in cells lacking Sec28. Wild-type (WT) yeast (BY4741), a class E *vps* mutant (*vps23*Δ), or *SEC28*-deficient cells (*sec28*Δ) bearing multicopy plasmids expressing *myc-SEC33* (pADH-SEC33) and *GFP-VPS27* (pGFP-VPS27) were lysed and subjected to immunoprecipitation as described for panel A. (C) A control protein, Vsm1, does not precipitate myc-Sec27. Wild-type yeast (BY4741) cells bearing multicopy plasmids expressing *myc-SEC27* (pADH-SEC27) or *myc-VSM1* (pADH-VSM1), together with a second plasmid expressing *GFP-VPS27* (pGFP-VPS27), were subjected to immunoprecipitation as described for panel A. Detection of the precipitated proteins in immunoblots was performed with anti-Vps27 (1:1,000) or anti-myc (1:1,000) antibodies. (D) Coimmunoprecipitation of Sec28-GFP with Vps27-myc expressed from the genome. Wild-type yeast (W303-1a) cells bearing integrated *SEC28-GFP* (GGY3), *VPS27-MYC* (GGY4), or both (GGY5) were lysed and subjected to immunoprecipitation. −, cells lacking the integration; +, cells bearing the integration of the corresponding tag. Detection of the precipitated proteins in immunoblots was performed with anti-GFP (1:1,000) or anti-myc (1:1,000) antibodies. Samples of the TCL are shown (50 μg protein/lane).

levels of myc-Sec21 were somewhat lower than those of the COPIb subunits, this may partly account for our inability to detect an interaction between Sec21 and Vps27.

To examine Vps27-COPIb complex formation at endogenous levels of protein expression, we integrated a myc tag at the 3′ end of *VPS27* and a GFP tag at the 3′ end of *SEC28* in wild-type cells. As shown in Fig. 5D, Vps27-myc was able to specifically precipitate Sec28-GFP when both were expressed from their native promoters. Vps27 binding to COPIB subcomplex components further supports our hypothesis of COPI involvement in the endosomal protein sorting pathway.

Partial colocalization between a COPIb subunit and Vps27. The physical interaction of GFP-Vps27 with COPIb subunits (Fig. 5) suggests that they colocalize at the intracellular level.

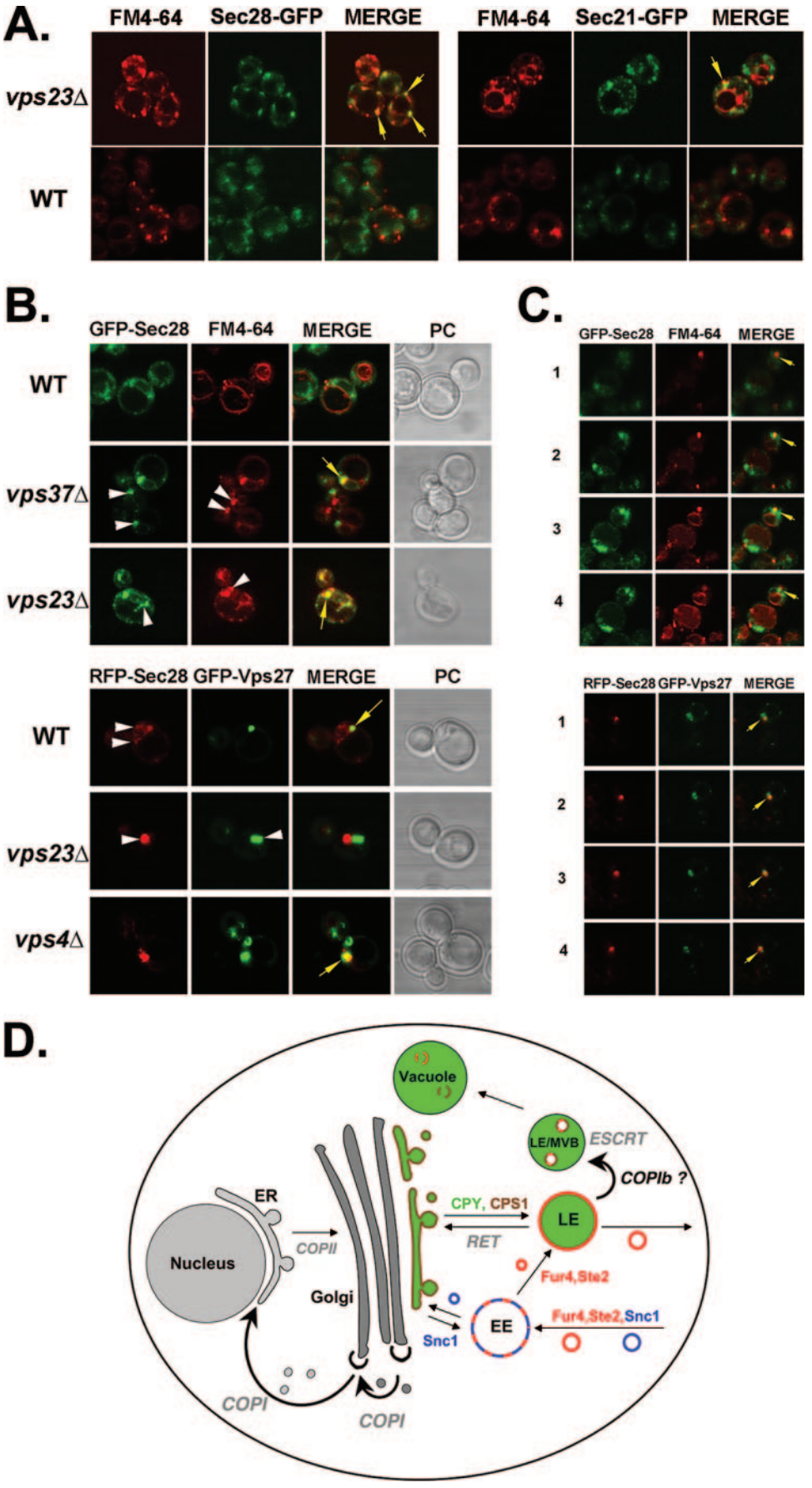
A.
FM4-64
Sec28-GFP
MERGE
FM4-64
Sec21-GFP
MERGE
vps23Δ
WT
B.
GFP-Sec28
FM4-64
MERGE
PC
WT
vps37Δ
vps23Δ
RFP-Sec28
GFP-Vps27
MERGE
PC
WT
vps23Δ
vps4Δ
C.
GFP-Sec28
FM4-64
MERGE
1
2
3
4
RFP-Sec28
GFP-Vps27
MERGE
1
2
3
4
D.
Vacuole
LE/MVB
ESCRT
COPIb ?
ER
CPY, CPS1
LE
RET
Nucleus
COPII
Golgi
Fur4,Ste2
EE
Fur4,Ste2,Snc1
Snc1
COPI
COPI

To test this, we examined the localization of Sec28 and Sec21 tagged at their carboxy termini with GFP and expressed from their genomic loci in wild-type cells and a class E *vps* mutant (*vps23*Δ cells). In *vps23*Δ cells, we observed punctate labeling for both proteins which partially colocalized with FM4-64, upon pulse-chase endosomal labeling (pulse performed on ice; short chase at 26°C) (Fig. 6A). In wild-type cells, however, the integrated forms of both Sec28-GFP and Sec21-GFP appeared to have a more diffuse pattern of localization than that observed in the *vps23*Δ mutant, and we did not observe definitive colocalization with FM4-64. The partial colabeling of Sec21-GFP with FM4-64 in *vps23*Δ cells may indicate that this COPIf component can also reside on endosomes. In addition, we followed the localization of Sec28 tagged at the amino terminus with GFP (GFP-Sec28) and expressed from a multicopy plasmid. GFP-Sec28 also colocalized in part with FM4-64 in the class E *vps* mutants (*vps37*Δ and *vps23*Δ cells) and gave a basically similar pattern of labeling (Fig. 6B, upper panels) to that seen for Sec28-GFP. These observations demonstrate that Sec28 resides, at least in part, on the endocytic pathway. Next, we assessed the colocalization of GFP-Vps27 and RFP-Sec28 expressed from multicopy plasmids in class E *vps* mutants (*vps4*Δ and *vps23*Δ cells) (Fig. 6B, lower panels). GFP-Vps27 typically labeled 1 or 2 large punctate structures (Fig. 6B, lower panels and reference 35), and we observed partial colocalization with RFP-Sec28 in 5 to 10% of cells (Fig. 6B, lower panels; see yellow arrow). We performed *z* sectioning of the cells showing colocalization to be sure that the colabeled compartments overlap (Fig. 6C). Indeed, Sec28 partially colocalized with both endosomal markers, FM4-64 (Fig. 6C, upper panels) and GFP-Vps27 (Fig. 6C, lower panels), in the *z* sections of these cells. We noted that in most other cells, the fluorescent RFP-Sec28 and GFP-Vps27 punctate structures were often found adjacent to one another in wild-type and *vps23*Δ cells (Fig. 6B, lower panels), as well as in *vps4*Δ cells (data not shown). This suggests that COPIb and Vps27 reside at closely juxtaposed compartments, which may confer their physical association under certain conditions.

DISCUSSION

The direct involvement of COPI in Golgi apparatus-ER retrograde transport and indirect involvement in anterograde ER-Golgi apparatus transport are well established in both yeast and mammals (40, 56). Earlier studies also suggested an involvement of COPI in endosomal protein sorting to MVBs and lysosomes in mammalian cells (1, 15, 29, 59). In this study, we propose that COPI facilitates endosomal protein sorting in *Saccharomyces cerevisiae* and provide evidence that certain components of the COPIB subcomplex are important for MVB protein sorting, which is required to deliver both biosynthetic and endocytosed membrane cargo to the vacuolar lumen (28, 34, 41). Class E *vps* mutants (i.e., *vps23*, *vps27*, etc.) are impaired in this transport pathway and are characterized by an enlarged late endosome, referred to as the class E compartment (47, 50). According to our observations, certain COPIb mutants (e.g., *sec27-1* and *sec28*Δ), like class E *vps* mutants (6, 50), secrete a portion of CPY (Fig. 1A, B, C, and E; and Table 3) and accumulate an enlarged late endosome/class E compartment labeled by FM4-64 (Fig. 4) in which membrane proteins destined to reach the vacuolar lumen (i.e., CPS1, Fur4, Ste2, and Ste3) accumulate (Fig. 2, 3A, and 4B). In *sec33-1* cells; however, we observed somewhat milder effects on endosomal protein sorting and FM4-64 labeling (Fig. 2 and 4). This may be due to defects in ER-Golgi apparatus transport, as described previously for *sec33-1* cells at permissive temperatures (60). Indeed, we also observed a deficiency in GFP-Snc1 plasma membrane localization in this mutant, unlike in *sec27-1* and *sec28*Δ cells (51). On the other hand, the interaction seen between myc-Sec33 and GFP-Vps27 (Fig. 5) implies the direct involvement of this αCOP ortholog in endosomal protein sort-

FIG. 6. Sec28 localizes to endosomal compartments labeled by FM4-64 and Vps27. (A) *SEC28-GFP* and *SEC21-GFP*, expressed from the genome, partially colocalize with FM4-64. Wild-type (WT) yeast (BY4741) and a class E mutant (*vps23*Δ) expressing intragenomic *SEC28-GFP* (Sec28-GFP; GGY3, and GGY6, respectively) and *SEC21-GFP* (Sec21-GFP; GGY7 and GGY8, respectively) were labeled with FM4-64 and examined by confocal microscopy. Arrows indicate the Sec28-GFP- and Sec21-GFP-labeled endosomal compartments in which FM4-64 accumulates. (B) The upper panels show overexpressed *GFP-SEC28* partially colocalizes with FM4-64 labeling of the endocytic pathway. Wild-type yeast cells (BY4741) and class E mutant cells (*vps23*Δ and *vps37*Δ) expressing *GFP-SEC28* from a multicopy plasmid (pADH-GFP-SEC28) were labeled with FM4-64 and examined by confocal microscopy. Arrows indicate GFP-Sec28-labeled class E compartments in which FM4-64 accumulates. The lower panel shows that GFP-Vps27 and RFP-Sec28 partially colocalize. Wild-type yeast cells (W303-1a) and mutant *vps23*Δ and *vps4*Δ cells expressing *RFP-SEC28* from a multicopy plasmid (pADH-RFP-SEC28) and *GFP-VPS27* expressed from a multicopy plasmid (pGFP-VPS27) were examined by confocal microscopy. An arrow indicates one of the colabeled endosomal compartments in these cells, while arrowheads point out juxtaposed RFP-Sec28- and GFP-Vps27-labeled compartments. Both phase-contrast microscopy (PC) and merged (MERGE) panels are indicated. (C) *z* sections of cells showing Sec28 colocalized with endosomal markers. The upper panels show class E mutant cells (*vps23*Δ) expressing *GFP-SEC28* from a multicopy plasmid (pADH-GFP-SEC28) were labeled with FM4-64 and examined by confocal microscopy. The lower panels show class E mutant cells (*vps23*Δ) expressing *RFP-SEC28* (pADH-RFP-SEC28) and *GFP-VPS27* (pGFP-VPS27) were examined by confocal microscopy. *z* sections were taken in increments of 0.5 μm. (D) A model for COPIb in endosomal protein sorting in yeast. Endocytosed membrane proteins Snc1 (blue) and Ste2 or Fur4 (red) is first targeted to the early endosome (red and blue circle) by carrier vesicles. Next, sorting of Snc1 to the *trans*-Golgi apparatus and Fur4 and Ste2 to the late (recycling) endosome occurs. Biosynthetic soluble cargo (i.e., CPY [green]) and membrane cargo (i.e., CPS1 [brown]) are sorted from the *trans*-Golgi apparatus to the late endosome (large red and brown circle) as well. MVB biogenesis and protein sorting therein are mediated in a COPIb- and ESCRT-dependent manner (see Discussion). During MVB biogenesis, intralumenal vesicles (small brown and red circles) are delivered to the vacuolar lumen where they are degraded. *COPI* indicates ER-Golgi and intra-Golgi apparatus retrograde transport steps regulated by this coat complex. *COPII* indicates the ER-Golgi apparatus anterograde transport steps regulated by this coat complex. *RET* indicates the retromer complex involved in late endosome-*trans*-Golgi recycling. Recycled Fur4 and, possibly, Ste2 are delivered to the plasma membrane by secretory vesicles derived from late endosomes.

ing. The participation of Sec33 in endocytic trafficking is also supported by studies performed with mammalian cells (29).

Using two different CPY secretion assays, we detected general defects in endosomal protein sorting in certain COPIb mutants (Fig. 1A, B, C, and E). While the results of these assays do not point out a specific defect in endosomal transport, subsequent studies utilizing fluorescent protein-tagged markers and the fluorescent dye FM4-64 suggest that a late step in vacuolar protein sorting is affected in COPIb mutants (Fig. 2, 3A, and 4). Earlier work in yeast supports this view, as GFP-Snc1 recycling from early endosomes to the Golgi apparatus is also affected in COPIb mutants, as shown by us recently (51). GFP-Snc1 was found to be more highly enriched on the bud plasma membrane in certain COPIb mutants and in an ESCRT mutant than in wild-type cells. This further illustrates a phenotypic similarity between the COPIb mutants (in particular *sec27-1* and *sec28*Δ) and the class E *vps* mutants (i.e., *vps28*Δ, *vps23*Δ, and *vps37*Δ cells) tested by us and leads us to suggest a role for COPIb in the late endosomal protein sorting. This is supported by ancillary studies in yeast that previously demonstrated impaired FM4-64 staining in *arf1* mutants and suggested a requirement for Arf1 in endosomal transport (25, 61). If Arf1 is also required for a post-Golgi function of COPI, as predicted from these studies, then its direct involvement in the MVB pathway should be examined. Thus, multiple lines of evidence implicate both Arf and COPI function in post-Golgi apparatus transport in yeast, as well as mammals.

To determine whether components of the MVB machinery and COPIb interact, we performed a pull-down assay between the MVB-associated protein, Vps27, and tagged COPIb subunits. We found that all COPIb components bind Vps27 in both wild-type cells and a *vps23*Δ mutant, suggesting that these proteins may form a complex in yeast (Fig. 5). However, Sec28 is probably not necessary for COPI-Vps27 complex formation (Fig. 5B). At this point, it does not appear that the COPIf subunit, Sec21, is able to interact with Vps27, although the low expression levels of this protein may have obscured the result (Fig. 5B).

In experiments designed to reveal whether components of the MVB machinery and COPI interact, we found partial colocalization between Sec28 and two endosomal markers, FM4-64 and GFP-Vps27 (Fig. 6B, lower panels). Colabeling was observed in a small number of cells (5 to 10%), while most others showed a close juxtaposition of Sec28 and either FM4-64- or Vps27-labeled compartments. This result may indicate that Sec28 is only loosely associated with endosomal compartments, which is supported by the low level of interaction seen between Vps27 and Sec28 in immunoprecipitation experiments (Fig. 5). Thus, we predict that certain COPI components act prior to MVB formation, perhaps, at the level of late endosome-MVB protein transport (see model in Fig. 6D). Further studies will be required to resolve this issue.

COPI is not the first vesicle coat shown to be required for multiple intracellular transport pathways. Earlier studies demonstrated that clathrin and clathrin adaptor proteins are responsible for transport between various secretory and endocytic compartments that bud vesicles from the plasma membrane, *trans*-Golgi apparatus, and endosomes (36, 37, 40, 42). Clathrin recruitment to membranes is determined by the specific type of adaptor protein involved. Among them are the classical clathrin adaptors AP1, AP2, AP3, and AP4 and alternate adaptors, like GGA and Hrs/Vps27 (40, 42). Interestingly, a distinct structural similarity between AP2, which mediates endocytosis, and the COPIf subcomplex was recently proposed (31, 40). Thus, COPI, like clathrin, may make use of alternate adaptor proteins (e.g., Vps27) to confer endosomal protein sorting.

Vps27 contains a FYVE domain that binds to PI(3)P on endosomal membranes (42) and a ubiquitin-interacting domain (UIM) that recognizes ubiquitinated cargoes destined for vacuolar lumen and sorts them into the intralumenal vesicles that form on the limiting membrane of MVBs. Vps27 also contains a clathrin-binding motif, and its mammalian homolog, Hrs, is a clathrin adaptor that binds directly to the β-propeller domain on clathrin (48). Such β-propeller domains (or WD-40 repeats) are also present in the Sec27 and Sec33 COPIb subunits (21, 40). The similar structural makeup between the clathrin-Hrs complex and the COPIb-Vps27 complex, described here, suggests that the latter may constitute a novel coat. In that case, Vps27 might function as an alternate adaptor (instead of COPIf) in the COPIb clathrin-like coat. While the role for a Vps27-COPIb interaction is not well understood, it may lead to the delivery of ubiquitinated cargo to Vps27 and subsequent MVB formation. Thus, we postulate a post-Golgi apparatus role for COPIb in the passage of cargo from late recycling endosomes into the MVB (Fig. 6D). These could be the same compartment, since the resolution of yeast endosomal compartments is somewhat limited.

According to morphological studies, class E *vps* mutants accumulate tubular or stacked membranes to constitute a compartment that either precedes or gives rise to the MVB (47). Assuming the existence of such a morphologically distinct endocytic compartment (Fig. 6B), we suggest that COPI could be needed for protein transport into MVBs. While the specific role of COPI in protein sorting to MVBs is not known, there are two likely possibilities. The "classical" view would be that COPI functions independently of the MVB machinery in the delivery of carrier vesicles (containing Fur4, Ste2, Ste3, and CPS1) from the late endosome to the MVB (see model, Fig. 6D). This view is supported by studies showing a distinct localization pattern for either Vps27 (a marker of MVBs) or Sec28 and only partial colocalization (Fig. 6B, lower panels). Moreover, the turnoff of *SEC28* expression in the *vps23*Δ mutant leads to enhanced CPY secretion (Fig. 1E), implying an additive synthetic effect. Alternatively, the role of COPIb might be different from the accepted role of COPI in vesicle biogenesis. Given the similar phenotype seen between ESCRT and certain COPIb mutants (Fig. 1 to 4 and see reference 51) and the physical interaction between Vps27 and Sec28 (Fig. 5), perhaps COPIb participates in intralumenal vesicle biogenesis and sorting on the limiting membrane of the MVB. The Vps27-COPIb complex may then facilitate cargo recognition and, thus, play a role in protein sorting to, or biogenesis of, the MVB. Based upon our experiments, however, we cannot exclude the alternate possibility that COPI is involved in the transport of components from early to late endosomes, which somehow restricts protein sorting into the MVB. Finally, COPI may be involved in multiple steps of endosomal transport, similar to what is proposed for the class E *vps* protein, Vps4 (62). Our study supports previous findings in mammalian cells and shows for the first time an involvement for COPIB sub-

complex components in late endosomal protein sorting in yeast.

ACKNOWLEDGMENTS

We are grateful to Scott Emr for helpful discussion. We thank Charles Barlowe, Kendall Blumer, Rainer Duden, Scott Emr, Olivier Deloche, Uttam Surana, Robert Piper, Mark Longtine, Andreas Mayer, Peter Novick, Howard Riezman, and Anne Spang for the generous gifts of reagents.

This work was supported by grants to J.E.G. by the Minna James Heineman and Minerva Foundations, Germany. J.E.G. holds the Henry Kaplan chair in Cancer Research.

REFERENCES

1. **Aniento, F., F. Gu, R. G. Parton, and J. Gruenberg.** 1996. An endosomal beta COP is involved in the pH-dependent formation of transport vesicles destined for late endosomes. J. Cell Biol. **133:**29–41.
2. **Babst, M., D. J. Katzmann, E. J. Estepa-Sabal, T. Meerloo, and S. D. Emr.** 2002. Escrt-III: an endosome-associated heterooligomeric protein complex required for mvb sorting. Dev. Cell **3:**271–282.
3. **Babst, M., D. J. Katzmann, W. B. Snyder, B. Wendland, and S. D. Emr.** 2002. Endosome-associated complex, ESCRT-II, recruits transport machinery for protein sorting at the multivesicular body. Dev. Cell **3:**283–289.
4. **Babst, M., G. Odorizzi, E. J. Estepa, and S. D. Emr.** 2000. Mammalian tumor susceptibility gene 101 (TSG101) and the yeast homologue, Vps23p, both function in late endosomal trafficking. Traffic **1:**248–258.
5. **Benichou, S., M. Bomsel, M. Bodeus, H. Durand, M. Doute, F. Letourneur, J. Camonis, and R. Benarous.** 1994. Physical interaction of the HIV-1 Nef protein with beta-COP, a component of non-clathrin-coated vesicles essential for membrane traffic. J. Biol. Chem. **269:**30073–30076.
6. **Bilodeau, P. S., J. L. Urbanowski, S. C. Winistorfer, and R. C. Piper.** 2002. The Vps27p Hse1p complex binds ubiquitin and mediates endosomal protein sorting. Nat. Cell Biol. **4:**534–539.
7. **Bonangelino, C. J., E. M. Chavez, and J. S. Bonifacino.** 2002. Genomic screen for vacuolar protein sorting genes in Saccharomyces cerevisiae. Mol. Biol. Cell **13:**2486–2501.
8. **Bowers, K., J. Lottridge, S. B. Helliwell, L. M. Goldthwaite, J. P. Luzio, and T. H. Stevens.** 2004. Protein-protein interactions of ESCRT complexes in the yeast Saccharomyces cerevisiae. Traffic **5:**194–210.
9. **Bowers, K., and T. H. Stevens.** 2005. Protein transport from the late Golgi to the vacuole in the yeast Saccharomyces cerevisiae. Biochim. Biophys. Acta **1744:**438–454.
10. **Bugnicourt, A., M. Froissard, K. Sereti, H. D. Ulrich, R. Haguenauer-Tsapis, and J. M. Galan.** 2004. Antagonistic roles of ESCRT and Vps class C/HOPS complexes in the recycling of yeast membrane proteins. Mol. Biol. Cell **15:**4203–4214.
11. **Burd, C. G., M. Peterson, C. R. Cowles, and S. D. Emr.** 1997. A novel Sec18p/NSF-dependent complex required for Golgi-to-endosome transport in yeast. Mol. Biol. Cell **8:**1089–1104.
12. **Conibear, E., and T. H. Stevens.** 2002. Studying yeast vacuoles. Methods Enzymol. **351:**408–432.
13. **Cosson, P., C. Demolliere, S. Hennecke, R. Duden, and F. Letourneur.** 1996. Delta- and zeta-COP, two coatomer subunits homologous to clathrin-associated proteins, are involved in ER retrieval. EMBO J. **15:**1792–1798.
14. **Couve, A., and J. E. Gerst.** 1994. Yeast Snc proteins complex with Sec9. Functional interactions between putative SNARE proteins. J. Biol. Chem. **269:**23391–23394.
15. **Daro, E., D. Sheff, M. Gomez, T. Kreis, and I. Mellman.** 1997. Inhibition of endosome function in CHO cells bearing a temperature-sensitive defect in the coatomer (COPI) component epsilon-COP. J. Cell Biol. **139:**1747–1759.
16. **Darsow, T., S. E. Rieder, and S. D. Emr.** 1997. A multispecificity syntaxin homologue, Vam3p, essential for autophagic and biosynthetic protein transport to the vacuole. J. Cell Biol. **138:**517–529.
17. **Deloche, O., B. G. Yeung, G. S. Payne, and R. Schekman.** 2001. Vps10p transport from the trans-Golgi network to the endosome is mediated by clathrin-coated vesicles. Mol. Biol. Cell **12:**475–485.
18. **Duden, R.** 2003. ER-to-Golgi transport: COP I and COP II function. Mol. Membr. Biol. **20:**197–207.
19. **Duden, R., M. Hosobuchi, S. Hamamoto, M. Winey, B. Byers, and R. Schekman.** 1994. Yeast beta- and beta′-coat proteins (COP). Two coatomer subunits essential for endoplasmic reticulum-to-Golgi protein traffic. J. Biol. Chem. **269:**24486–24495.
20. **Duden, R., L. Kajikawa, L. Wuestehube, and R. Schekman.** 1998. epsilon-COP is a structural component of coatomer that functions to stabilize alpha-COP. EMBO J. **17:**985–995.
21. **Eugster, A., G. Frigerio, M. Dale, and R. Duden.** 2004. The alpha- and beta′-COP WD40 domains mediate cargo-selective interactions with distinct di-lysine motifs. Mol. Biol. Cell **15:**1011–1023.
22. **Eugster, A., G. Frigerio, M. Dale, and R. Duden.** 2000. COP I domains required for coatomer integrity, and novel interactions with ARF and ARF-GAP. EMBO J. **19:**3905–3917.
23. **Faure, J., R. Stalder, C. Borel, K. Sobo, V. Piguet, N. Demaurex, J. Gruenberg, and D. Trono.** 2004. ARF1 regulates Nef-induced CD4 degradation. Curr. Biol. **14:**1056–1064.
24. **Galan, J.-M., A. Wiederkehr, J. H. Seol, R. Haguenauer-Tsapis, R. J. Deshaies, H. Riezman, and M. Peter.** 2001. Skp1p and the F-box protein Rcy1p form a non-SCF complex involved in recycling of the SNARE Snc1p in yeast. Mol. Cell. Biol. **21:**3105–3117.
25. **Gaynor, E. C., C. Y. Chen, S. D. Emr, and T. R. Graham.** 1998. ARF is required for maintenance of yeast Golgi and endosome structure and function. Mol. Biol. Cell **9:**653–670.
26. **Gaynor, E. C., and S. D. Emr.** 1997. COPI-independent anterograde transport: cargo-selective ER to Golgi protein transport in yeast COPI mutants. J. Cell Biol. **136:**789–802.
27. **Gruenberg, J., and F. R. Maxfield.** 1995. Membrane transport in the endocytic pathway. Curr. Opin. Cell Biol. **7:**552–563.
28. **Gruenberg, J., and H. Stenmark.** 2004. The biogenesis of multivesicular endosomes. Nat. Rev. Mol. Cell Biol. **5:**317–323.
29. **Gu, F., F. Aniento, R. G. Parton, and J. Gruenberg.** 1997. Functional dissection of COP-I subunits in the biogenesis of multivesicular endosomes. J. Cell Biol. **139:**1183–1195.
30. **Gu, F., and J. Gruenberg.** 2000. ARF1 regulates pH-dependent COP functions in the early endocytic pathway. J. Biol. Chem. **275:**8154–8160.
31. **Hoffman, G. R., P. B. Rahl, R. N. Collins, and R. A. Cerione.** 2003. Conserved structural motifs in intracellular trafficking pathways: structure of the gammaCOP appendage domain. Mol. Cell **12:**615–625.
32. **Hosobuchi, M., T. Kreis, and R. Schekman.** 1992. SEC21 is a gene required for ER to Golgi protein transport that encodes a subunit of a yeast coatomer. Nature **360:**603–605.
33. **Katzmann, D. J., M. Babst, and S. D. Emr.** 2001. Ubiquitin-dependent sorting into the multivesicular body pathway requires the function of a conserved endosomal protein sorting complex, ESCRT-I. Cell **106:**145–155.
34. **Katzmann, D. J., G. Odorizzi, and S. D. Emr.** 2002. Receptor downregulation and multivesicular-body sorting. Nat. Rev. Mol. Cell Biol. **3:**893–905.
35. **Katzmann, D. J., C. J. Stefan, M. Babst, and S. D. Emr.** 2003. Vps27 recruits ESCRT machinery to endosomes during MVB sorting. J. Cell Biol. **162:**413–423.
36. **Kirchhausen, T.** 2000. Clathrin. Annu.Rev. Biochem. **69:**699–727.
37. **Le Roy, C., and J. L. Wrana.** 2005. Clathrin- and non-clathrin-mediated endocytic regulation of cell signalling. Nat. Rev. Mol. Cell Biol. **6:**112–126.
38. **Letourneur, F., E. C. Gaynor, S. Hennecke, C. Demolliere, R. Duden, S. D. Emr, H. Riezman, and P. Cosson.** 1994. Coatomer is essential for retrieval of dilysine-tagged proteins to the endoplasmic reticulum. Cell **79:**1199–1207.
39. **Longtine, M. S., A. McKenzie III, D. J. Demarini, N. G. Shah, A. Wach, A. Brachat, P. Philippsen, and J. R. Pringle.** 1998. Additional modules for versatile and economical PCR-based gene deletion and modification in Saccharomyces cerevisiae. Yeast **14:**953–961.
40. **McMahon, H. T., and I. G. Mills.** 2004. COP and clathrin-coated vesicle budding: different pathways, common approaches. Curr. Opin. Cell Biol. **16:**379–391.
41. **Odorizzi, G., M. Babst, and S. D. Emr.** 1998. Fab1p PtdIns(3)P 5-kinase function essential for protein sorting in the multivesicular body. Cell **95:**847–858.
42. **Owen, D. J., B. M. Collins, and P. R. Evans.** 2004. Adaptors for clathrin coats: structure and function. Annu. Rev. Cell Dev. Biol. **20:**153–191.
43. **Padmashree, C. G., and U. Surana.** 2001. Cdc28-Clb mitotic kinase negatively regulates bud site assembly in the budding yeast. J. Cell Sci. **114:**207–218.
44. **Pepperkok, R., J. Scheel, H. Horstmann, H. P. Hauri, G. Griffiths, and T. E. Kreis.** 1993. Beta-COP is essential for biosynthetic membrane transport from the endoplasmic reticulum to the Golgi complex in vivo. Cell **74:**71–82.
45. **Piper, R. C., N. J. Bryant, and T. H. Stevens.** 1997. The membrane protein alkaline phosphatase is delivered to the vacuole by a route that is distinct from the VPS-dependent pathway. J. Cell Biol. **138:**531–545.
46. **Piper, R. C., and J. P. Luzio.** 2001. Late endosomes: sorting and partitioning in multivesicular bodies. Traffic **2:**612–621.
47. **Prescianotto-Baschong, C., and H. Riezman.** 2002. Ordering of compartments in the yeast endocytic pathway. Traffic **3:**37–49.
48. **Raiborg, C., K. G. Bache, A. Mehlum, E. Stang, and H. Stenmark.** 2001. Hrs recruits clathrin to early endosomes. EMBO J. **20:**5008–5021.
49. **Raths, S., J. Rohrer, F. Crausaz, and H. Riezman.** 1993. end3 and end4: two mutants defective in receptor-mediated and fluid-phase endocytosis in Saccharomyces cerevisiae. J. Cell Biol. **120:**55–65.
50. **Rieder, S. E., L. M. Banta, K. Kohrer, J. M. McCaffery, and S. D. Emr.** 1996. Multilamellar endosome-like compartment accumulates in the yeast vps28 vacuolar protein sorting mutant. Mol. Biol. Cell **7:**985–999.
51. **Robinson, M., P. P. Poon, C. Schindler, L. E. Murray, R. Kama, G. Gabriely, R. A. Singer, A. Spang, G. C. Johnston, and J. E. Gerst.** 2006. The Gcs1 Arf-GAP mediates Snc1,2 v-SNARE retrieval to the Golgi in yeast. Mol. Biol. Cell **17:**1845–1858.

52. **Rose, M. D., F. Winston, and P. Hieter.** 1990. Methods in yeast genetics. Cold Spring Harbor Laboratory Press, Cold Spring Harbor, NY.
53. **Roth, M. G.** 1999. Snapshots of ARF1: implications for mechanisms of activation and inactivation. Cell **97:**149–152.
54. **Semenza, J. C., K. G. Hardwick, N. Dean, and H. R. Pelham.** 1990. ERD2, a yeast gene required for the receptor-mediated retrieval of luminal ER proteins from the secretory pathway. Cell **61:**1349–1357.
55. **Shih, S. C., D. J. Katzmann, J. D. Schnell, M. Sutanto, S. D. Emr, and L. Hicke.** 2002. Epsins and Vps27p/Hrs contain ubiquitin-binding domains that function in receptor endocytosis. Nat. Cell Biol. **4:**389–393.
56. **Spang, A.** 2002. ARF1 regulatory factors and COPI vesicle formation. Curr. Opin. Cell Biol. **14:**423–427.
57. **Stefan, C. J., and K. J. Blumer.** 1999. A syntaxin homolog encoded by VAM3 mediates down-regulation of a yeast G protein-coupled receptor. J. Biol. Chem. **274:**1835–1841.
58. **Vida, T. A., and S. D. Emr.** 1995. A new vital stain for visualizing vacuolar membrane dynamics and endocytosis in yeast. J. Cell Biol. **128:**779–792.
59. **Whitney, J. A., M. Gomez, D. Sheff, T. E. Kreis, and I. Mellman.** 1995. Cytoplasmic coat proteins involved in endosome function. Cell **83:**703–713.
60. **Wuestehube, L. J., R. Duden, A. Eun, S. Hamamoto, P. Korn, R. Ram, and R. Schekman.** 1996. New mutants of Saccharomyces cerevisiae affected in the transport of proteins from the endoplasmic reticulum to the Golgi complex. Genetics **142:**393–406.
61. **Yahara, N., T. Ueda, K. Sato, and A. Nakano.** 2001. Multiple roles of Arf1 GTPase in the yeast exocytic and endocytic pathways. Mol. Biol. Cell **12:** 221–238.
62. **Zahn, R., B. J. Stevenson, S. Schroder-Kohne, B. Zanolari, H. Riezman, and A. L. Munn.** 2001. End13p/Vps4p is required for efficient transport from early to late endosomes in Saccharomyces cerevisiae. J. Cell Sci. **114:**1935–1947.